CONF-8808146--15

CHIRPING FOR EFFICIENCY ENHANCEMENT OF THE FREE-ELECTRON LASER*

Gerald T. Moore and John C. Goldstein†

Center for Advanced Studies and
Department of Physics and Astronomy
University of New Mexico
Albuquerque, New Mexico 87131, USA

CONF-8808146--15

DE89 007433

ABSTRACT

One-dimensional numerical studies have been made of free-electron laser oscillators in which the incident electron energy varies (chirps) as a function of time over each micropulse. Optical radiation resonant with such micropulses is chirped in frequency. Highest calculated efficiency (up to 8.1% for wavelengths near 10 μm) has been obtained in cases where the optical pulse at saturation is short compared to the slippage.

10th International Free Electron Laser Conference, Jerusalem, 1988

* Research supported by the Division of Advanced Energy Projects, U. S. Department of Energy.

† Permanent address: Group X-1, MS E531, Los Alamos National Laboratory, University of California, Los Alamos NM 87545, USA.

FG04-87ER13788

I. INTRODUCTION

In two recent publications [1,2] we developed a theoretical description of a short-pulse free-electron laser in which both the electron energy and the laser frequency vary (chirp) as a function of time over the micropulses. Such a chirped-pulse FEL would be powered by an RF linac in which the electrons are accelerated on the high-gradient phase of the RF field. The chirped electron pulses emerging from the accelerator would pass through and be compressed by the field of achromatic bending magnets as they are injected into the wiggler.

If the FEL produces coherent radiation near a single time-dependent frequency $\omega_s(\tau)$ and its harmonics, where $\tau = t - z/c$ is retarded time, then the trajectory $\tau(z,\tau_0)$ of resonant particles (i.e., fictitious particles which move at the speed of the ponderomotive potential) is given by

$$\int_{\tau_0}^{\tau} d\tau' \omega_s(\tau') = \int_0^z dz' k_q(z'), \tag{1}$$

where τ_0 is the time of injection into the wiggler and k_q is the wave vector of the (possibly tapered) wiggler. The trajectories $\tau(z,\tau_0)$ are nonintersecting and monotonically increasing in z. The velocity $v_z(z,\tau)$ of these trajectories is given by

$$1/v_z(z,\tau) - 1/c = k_q(z)/\omega_s(\tau), \tag{2}$$

which in the extreme relativistic limit corresponds to the Doppler upshift condition

$$\gamma_r^2(z,\tau) = \omega_s(\tau)\Delta(z)/2ck_q(z). \tag{3}$$

Here $mc^2\gamma_r(z,\tau)$ is the resonant electron energy, and the mass shift

$$\Delta(z) = 1 + e^2 A_q^2(z)/m^2c^2 \tag{4}$$

accounts for the fact that some of the electron energy is converted to transverse motion inside the wiggler. $A_q(z)$ is the RMS amplitude of the wiggler vector potential. In order for electrons to interact strongly with the laser field, they must be close to resonance. Except in special cases, the resonant particle trajectories are accelerated, so that electrons stay close to resonance only by becoming trapped in the wells of the ponderomotive potential. In order that they become trapped at the wiggler entrance, their incident energies should be close to $mc^2\gamma_r(0,\tau)$, as given by Eq. (3). This provide a criterion for choosing the carrier frequency $\omega_s(\tau)$.

Efficiency enhancement by wiggler tapering [3] is accomplished by decreasing Δ or increasing k_q adiabatically as a function of z, such that electrons remain trapped and close in energy to a decreasing γ_r. Given an intense optical pulse with a decreasing frequency $\omega_s(\tau)$, one could equally well enhance the efficiency, even with a uniform wiggler, by taking advantage of the fact that electrons slip to larger value of τ as they traverse the wiggler. These considerations motivated us to undertake a one-dimensional numerical study of short-pulse propagation in the chirped-pulse FEL oscillator. The results so far have been encouraging as regards efficiency enhancement, but not in accord with the idea of adiabatic energy extraction from trapped electrons. Instead, our best results have been obtained when the optical pulse is short compared to the slippage between light and electrons, so that individual electrons interact strongly with the light only over a short fraction of the wiggler length.

Our theoretical approach is based on the slowly-varying envelope (SVA) approximation, whereby the laser field $\hat{E}_s(z,\tau)$ is written (neglecting higher harmonics) as a product

$$\hat{E}_s(\tau) = E_s(z,\tau)e^{-i\phi(\tau)}, \tag{5}$$

where $d\phi/d\tau = \omega_s(\tau)$. We presume that ω_s can be appropriately chosen such that E_s varies little over an optical period. The SVA approximation is almost universally

used in FEL theory, although ω_s is usually taken to be constant. The amplitude E_s is calculated self-consistently by numerically solving the coupled Maxwell and electron equations for many passes through the resonator. The validity of the SVA approximation becomes questionable, however, when the time derivative of the phase of the complex amplitude E_s becomes comparable to ω_s at times when the laser power is high or when the optical pulse becomes only a few periods long. Since these conditions develop in the situations where we obtain high-efficiency, our results in this regime are encouraging, but not conclusive. These conditions occur even without electron energy chirping or wiggler tapering. However, chirping, particularly when combined with inverse tapering, substantially increases the efficiency.

The dynamical equations for the chirped-pulse FEL have been presented elsewhere [1,2]. For present purposes we restrict these equations by assuming that higher harmonics can be neglected, that the electrons are ultrarelativistic, that there is no electron energy spread uncorrelated with time, and that the amplitude of the wiggler vector potential is untapered. We assume, furthermore, that the optical resonator is dispersionless. The dynamical equations become:

$$\sigma^*(z,\tau)\frac{\partial}{\partial z}[\sigma(z,\tau)E_s(z,\tau)] = \frac{e}{2mc}\frac{\omega_s(\tau)}{\omega_s(\tau_0)}\frac{A_q}{\gamma_r(z,\tau)} \times I(\tau_0)\frac{1}{2\pi}\int_0^{2\pi} d\theta_0 \exp[-i\theta(z,\tau_0,\theta_0)], \tag{6}$$

$$\frac{\partial\theta(z,\tau_0,\theta_0)}{\partial z} = 2k_q(z)[\gamma(z,\tau_0,\theta_0)/\gamma_r(z,\tau) - 1], \tag{7}$$

$$\frac{\partial\gamma(z,\tau_0,\theta_0)}{\partial z} = -\frac{1}{2c\gamma_r(z,\tau)}\frac{e^2}{m^2c^2}\{A_q E_s^*(z,\tau) \times \exp[-i\theta(z,\tau_0,\theta_0)] + c.c.\}. \tag{8}$$

Here θ is the electron phase angle in the ponderomotive potential, with initial value θ_0, A_q is the RMS wiggler vector potential (multiplied, except in Eq. (4), by a well-known difference of Bessel functions [4] if the wiggler is linearly polarized); and $I(\tau_0)$ is the incident electron current. The variables z, τ_0, and τ are related by Eq. (1). the complex function $\sigma(z,\tau)$ is obtained [5] by projecting the three-dimensional laser field onto the fundamental Gaussian mode of the resonator, so as to account for diffractive beam spreading and phase shift. Since the Gaussian beam waist depends on frequency, and the frequency ω_s depends on τ, σ becomes a function of τ for the chirped-pulse FEL. It is given by

$$\sigma(z,\tau) = \left[\frac{\pi\epsilon_0 c^2 Z_R}{\omega_s(\tau)}\right]^{\frac{1}{2}} \left[1 + \frac{i(z-z_0)}{Z_R}\right], \tag{9}$$

where Z_R is the Rayleigh range and z_0 is the coordinate of the beam waist. The laser power is $|\sigma E_s|^2$.

Equations (6)-(8) were obtained by multiple-scaling arguments along the lines of Ref. [4] and [5]. These arguments lead to the phase average over θ_0 in Eq. (6). The SVA approximation emerges naturally from the multiple-scaling analysis, and a breakdown of the SVA approximation may indicate a breakdown of the entire multiple-scaling perturbation procedure.

We assume that electron motion on the time scale of the pulse envelopes is determined by Eq. (1). When the resonant-particle trajectories are accelerated, only trapped electrons actually remain close to these trajectories. However, untrapped electrons move out of resonance and then do not radiate significantly at the laser frequency. Therefore, it should not be important to track them accurately. However, the large and essentially random phases of such electrons do contribute noise to our numerical simulations.

Equation (1) can be written as $\phi - \phi_0 = \psi$, where ψ is the wiggler phase, ϕ is the optical phase, and ϕ_0 is the initial value of the optical phase. Our numerical

integration procedure uses independent variables proportional to these phase angles, rather than z, τ, and τ_0. The latter, however, are used for output. The independent variables are defined on uniform grids, though the step size in ψ can differ from the step size in ϕ and ϕ_0. When different step sizes are used, three-point interpolation is used to relate values on the two grids. The fundamental dependent variables of the numerical computations are θ, γ, and the modulus and phase of the dimensionless complex amplitude

$$\tilde{E}_s(\psi,\phi) = [mc^2\omega_s(\phi)]^{-1/2}\sigma(\psi,\phi)E_s(\psi,\phi). \tag{10}$$

Since the phase of σ is independent of ϕ, there is no important distinction between the phase of E_s and the phase of $\tilde{E}_s$.

Although using the phase angles ψ, ϕ, ϕ_0 as independent variables greatly simplifies the integration of the dynamical equations across the wiggler, one pays a price in accounting for cavity-length detuning. As has been understood since the first FEL pulse calculations [6], laser lethargy effectively slows down the optical pulses in the FEL. If the cavity round-trip time at the vacuum speed of light is synchronized with the injection period of the the electron micropulses, one finds that the light lags behind the electrons after a number of passes, and the gain eventually goes below threshold. The usual way to compensate for lethargy is to shorten the optical cavity slightly. Typically the shortening ℓ is a few microns. The optical pulse is pushed forward in τ by an amount $\delta\tau = 2\ell/c$. For simulations of the chirped-pulse FEL this procedure must be combined with an interpolation to redefine the field on a uniform grid in ϕ. We do this by means of cubic splines. Before carrying out the spline fit, we make sure that the modulus of $\tilde{E}_s$ is positive at each point (by adding π to the phase if necessary) and then require that increments in the phase of $\tilde{E}_s$ between successive points be as small as possible (by adding or subtracting multiples of 2π). Usually the modulus and phase of $\tilde{E}_s$ are smoother

and less oscillatory than the real and imaginary parts of $\tilde{E}_s$, and so are better suited for interpolation.

A new feature of the chirped-pulse FEL in that shortening the optical cavity tends to push the optical field off resonance. The entire field, and not just the SVA, is pushed forward. In terms of the variables z and τ, the cavity detuning has the effect

$$R\sigma(L,\tau+\delta\tau)E_s(L,\tau+\delta\tau)\exp\left[-i\int_{\tau}^{\tau+\delta\tau}d\tau'\omega_s(\tau')\right] \xrightarrow[\text{next pass}]{} \sigma(0,\tau)E_s(0,\tau), \tag{11}$$

where L is the wiggler length and R is the amplitude reflection coefficient for the resonator. The frequency pushing effect is cumulative over many passes, and tends to make E_s less and less slowly varying. This is counteracted by the gain process, which produces new radiation near resonance as cavity losses attenuate the old radiation. However, we find that the chirped-pulse FEL usually does not work well with large ℓ ($\sim 10\mu m$). Instead, efficient operation is obtained with cavity detunings on the order of $0.5\mu m$.

II. NUMERICAL SIMULATIONS

Many of the simulation parameters we have used were chosen to approximate the Los Alamos FEL. The following parameters are invariant in the calculations presented here.

The wiggler is linearly polarized and has $N = 37$ periods. The wiggler vector potential is held constant, and the RMS wiggler field at the wiggler entrance is 0.21213T. The wiggler is tapered according to

$$k_q(z) = k_0(1+\alpha_q k_0 z/2\pi N)^{-\epsilon_q}, \tag{12}$$

where $2\pi/k_0 = 2.73cm$.

We take the laser field to be chirped either according to the power-law relation

$$\omega_s(\tau) = \omega_0(1 + \alpha_s\omega_0\tau/2\pi N)^{-\epsilon_s} \tag{13}$$

or the error-function relation

$$\omega_s(\tau) = \omega_0\left(\frac{1-\alpha_s}{1+\alpha_s\mathrm{erf}[(\tau-\tau_c)/T_c]}\right)^{\epsilon_s}, \tag{14}$$

where $2\pi c/\omega_0 = 10\mu m$. The Rayleigh range is $Z_R = 0.63m$ and the beam waist is located at $z_0 = 0.50505m$ from the wiggler entrance. The amplitude reflection coefficient of the cavity is $R = 0.98$ (i.e., 4% losses per pass). The electron current is assumed to be a Gaussian,

$$I(\tau_0) = I_0\exp\{-[(\tau_0-\tau_e)/T_e]^2\}, \tag{15}$$

with $I_0 = 100A$. Two cases will be considered, a long pulse ($\tau_e = 19psec$, $T_e = 6.171psec$) and a short pulse ($\tau_e = 2psec$, $T_e = 0.62psec$). The length of the short pulse is comparable to the slippage. In general the slippage $\tau(L,\tau_0) - \tau_0$ varies somewhat over the pulse. For the unchirped case it is $2\pi N/\omega_0 = 1.23psec$. The electrons at each τ_0 point are represented by 15 electrons on a uniform grid in θ_0. A small random jitter of θ_0 about the uniform grid points can be used to simulate noise. We define δ to be the full-width of the jitter as a fraction of the grid spacing $2\pi/15$.

The injected field on pass one is taken to be a Gaussian,

$$\sigma(0,\tau)E_s(0,\tau) = A_0[mc^2\omega_s(0)]^{\frac{1}{2}}\exp\{-[(\tau-\tau_s)/T_s]^2\}. \tag{16}$$

If we let the energy of the incident electrons define resonance, the computer program allows the input field to be detuned from resonance to the frequency

$$\omega(\tau) = \omega_s(\tau)(1 - \mu/2\pi N). \tag{17}$$

In practice this detuning is simulated by an oscillation of the wiggler amplitude. In the cw limit without chirping or tapering, and for $Z_R \gg L$, one expects maximum small-signal gain at $\mu = 2.6$. In general, however, the detuning giving maximum gain depends on the circumstances, and may even be negative (see Fig. 1). Although for numerical reasons A_0 cannot be set equal to zero, it can, if desired, be made so small that emission on the first pass is dominated by noise in the values of θ_0.

As a general rule, small-signal gain is highest when untrapped electrons remain near resonance, which occurs when the resonant particles are unaccelerated. This is the case if and only if we choose $\epsilon_q = \epsilon_s = 1$ and $\alpha_q = \alpha_s$ in Eqs. (12) and (23). Equation (1) then has the solution

$$\tau = \tau_0 + (1/\omega_0 + \alpha\tau_0/2\pi N)k_0 z. \tag{18}$$

As we shall see, the case $\alpha = .1$ has given the highest efficiency so far calculated for the chirped-pulse FEL.

Lethargy is mainly a problem during the start-up of the chirped-pulse FEL. There is little lethargy after saturation, since the electrons become bunched very quickly. If one starts with a small-signal optical pulse near resonance and with good overlap to the electron pulses, the gain on the first few passes can be very high, but soon the optical pulse falls to the rear of the electron pulses and the gain decreases. Usually it is not possible to shorten the cavity (increase ℓ) sufficiently to keep the light from falling to the back of the electron pulses without pushing the optical pulse off resonance. One exception is when one or both ends of the pulse are unchirped, as in Eq. (14). Then, with a 10 or 15 μm detuning, one can get lasing at two different frequencies at the ends of the electron pulses. However, there is no

lasing in the chirped region, even if the current peaks there. If one lengthens the cavity after saturation to $\ell = 0$, the chirped region begins to lase.

The results shown in Fig. 2 are for a short pulse with an error-function chirp ($\epsilon_s = 2, \alpha_s = 0.02, \tau_c = 2.4psec, T_c = 0.3psec, \alpha_q = 0$). The cavity was shortened by $15\mu m$ for the first 40 passes, then set back to $\ell = 0$. The small-signal gain on pass 8 reached 74%. The efficiency on pass 280 is 5.0%. This is pretty good, although we have done as well without any chirping. The dip in efficiency prior to pass 40 can be attributed to decreased lethargy at saturation. The cavity detuning is then pushing the optical pulse forward too fast.

In the strong-signal regime the optical pulse tends to break up into a series of sharp spikes. This behavior in the unchirped FEL is called the sideband instability [7,8], because it is manifested has a low-frequency sideband in the optical spectrum. This name seems inappropriate for the chirped FEL, which has a wide bandwidth whether or not this instability develops. Unfortunately this wide bandwidth precludes the use of spectral filtering to get rid of the spiking. Spiking tends to cause electron detrapping, and is the principal reason why we have not so far succeeded in (numerically) operating the chirped-pulse FEL in the trapped-particle regime.

As an example of spiking, Fig. 3 shows the pulse from Fig. 2 at the end of pass 280. The optical pulse has developed into an 11 GW spike with several smaller trailing spikes. The optical pulse energy ($2.85 \times 10^{-3} J$) exceeds the incident electron pulse energy ($2.28 \times 10^{-3} J$). The efficiency per bin peaks at about 9%. Note that efficiency per bin does not weight the amount of current actually injected at time τ_0. The resonant wave number $\omega_s(\tau)/c$ and the actual wave number are shown in solid and dashed lines, respectively. The latter, which incorporates the numerically calculated time derivative of the phase of E_s, shows a very jagged structure, which is characteristic of the strongly saturated regime. The trailing features in the optical pulse, especially the frequency in regions where the power is very small, are believed

to be numerical "noise," but the main peaks in the power appear to be "real." Note that the main spike is narrow compared to the current pulses.

We have carried out a series of computer experiments for linear wavelength chirp and taper ($\epsilon_s = \epsilon_q = 1$) for the short electron pulse. In most of the experiments ℓ is of the order of $0.5\mu m$. A common feature of these experiments is that the optical pulse builds up on the rear of the electron pulse. When it reaches a sufficient power level, it begins moving forward because of the positive value of ℓ. As it approaches maximal overlap with the electrons, the efficiency peaks. At this point the optical pulse consists of a very short high-power spike, followed by several small trailing spikes. Thereafter the pulse ceases to move forward, and there is often a decrease in the efficiency. The spikes are much shorter than the slippage, so that electrons do not stay trapped throughout the wiggler.

Either chirping or tapering alone tend to reduce the small-signal gain. However, in the special case $\alpha_s = \alpha_q$, where the resonant particles are unaccelerated, the gain is not reduced substantially. Note that positive α_q corresponds to inverse tapering of the wiggler. Combining positive α_s with negative α_q adversely affects the gain and efficiency, though it increases the tolerance of the FEL to cavity shortening. We attribute this increase to the radiation of higher frequencies at the back end of the optical pulse by untrapped electrons near the wiggler exit. Table 1 summarizes calculations for various combinations of α_s, α_q, ℓ, A_0, and δ. In all cases A_0 is sufficiently small that one starts in the small-signal regime. We take $\tau_s = 2.3psec$, $T_s = 0.85psec$, and $\mu = 3$. Figure 4 shows the evolution of the efficiency as a function of pass number for some of the computer experiments in Table 1.

Our calculations so far certainly do not represent a thorough exploration of the parameter space, and one can never be sure what would have happened in any experiment if more passes had been calculated. However, the following conclusions seem to be justified. First, lethargy rapidly erodes the small-signal gain if one

starts with an optical pulse near resonance. A $0.5\mu m$ cavity detuning has little effect on this erosion. The optical pulse moves forward after saturation, but the gain continues to decrease even though the overlap between optical and electron pulses is improving. The largest small-signal gain is obtained when $\alpha_s = \alpha_q$. We obtained the highest efficiency (8.13%) when $\alpha_s = \alpha_q = 0.1$.

The results obtained at saturation can depend on the optical pulse (or noise level) used to initiate the build-up of lasing. This is a bit surprising in view of the large amplification. For the "best case" just mentioned the pulse energy increases by a factor of 2.6×10^8 in 279 passes. Since the optical pulse gets shorter, the peak power is amplified even more. However, the optical pulse does not reach a steady-state prior to saturation. When we repeated this calculation starting from noise, the efficiency reached 5.85% or 6.56%, depending on the noise level. Frequency jitter associated with the noise is then always present at the front of the optical pulse. While experimental devices presumably will start from the shot noise associated with incoherent emission, it is unclear how well our simulations represent this noise. Details of the pulse evolution for our "best case" are shown in Figs. 5-7.

III. DISCUSSION

We have shown that combining frequency chirping with inverse wiggler tapering according to $\alpha_s = \alpha_q > 0$ enhances the efficiency of the FEL. However, even the case $\alpha_s = \alpha_q = 0$ can yield an efficiency above 5%, assuming an electron pulse length comparable to the slippage. In either case the resonant particles are unaccelerated. Electron trapping is not maintained throughout the wiggler. Saturation under these conditions is expected to occur when electons undergo about half an oscillation in the ponderomotive potential. For a cw FEL this corresponds to a maximum efficiency of $1/2N = 1.35\%$. However, when the electrons interact with an optical spike short compared to the slippage and consisting of N_s optical periods, they undergo half an oscillation while traversing N_s wiggler periods, so that

the maximum efficiency is $\eta = 1/2N_s$. To get a crude estimate of N_s, suppose that the dimensionless amplitude $a_s = eA_s/mc$ of the laser pulse vector potential is independent of τ over the N_s optical periods and is real and positive. The spatial frequency of synchrotron oscillations is $2k_q(a_s a_q/\Delta)^{1/2}$, where $a_q = eA_q/mc$. In order that the electrons undergo half a synchrotron oscillation while propagating through the interaction distance $2\pi N_s/k_q$, we would like

$$4N_s(a_s a_q/\Delta)^{1/2} = 1. \tag{19}$$

In general one cannot satisfy Eq. (19) for all of the electrons because of the z dependence of a_s associated with the optical beam focusing. For simplicity let us suppose that the Rayuleigh range Z_R is long compared to the wiggler, so that this is not a problem.

Since the laser field E_s is relatd to a_s according to

$$E_s = (mc\omega_s/e)a_s \tag{20}$$

in the SVA approximation, we can use Eq. (9) to write the laser power as

$$P_s = |\sigma E_s|^2 = (Z_R/4r_e)mc^2\omega_s(\tau)a_s^2, \tag{21}$$

where $r_e = e^2/4\pi\epsilon_0 mc^2$ is the clasical radius of the electron and ω_s is to be evaluated at the time of the optical pulse. The optical pulse energy is

$$\mathcal{E}_s = (\pi Z_R/2r_e)mc^2 N_s a_s^2. \tag{22}$$

The energy extracted from the electrons is $\mathcal{E}_e/2N_s$, where $\mathcal{E}_e$ is the energy in the electron pulse slipped over by the optical pulse. The strong-signal gain G, which at saturation is equal to the losses, is given by

$$G = \mathcal{E}_e / 2N_s \mathcal{E}_s . \tag{23}$$

Combining Eqs. (19), (22), and (23), we obtain the efficiency

$$\eta = 1/2N_s = 8\frac{a_q}{\Delta}\left(\frac{\mathcal{E}_e}{mc^2}\frac{r_e}{\pi Z_R}\frac{1}{G}\right)^{1/2} . \tag{24}$$

As Z_R decreases past the point where it is comparable to the propagation distance needed for the electron and optical pulses to slip by each other (which we have taken to be comparable to the wiggler length L), we expect Eq. (24) to no longer be valid, and η should peak and then decrease. The electron pulse energy $\mathcal{E}_e$ is of the order of the number of electrons per second (I/e) times the electron energy $(mc^2\gamma)$ times the electron pulse duration $(\Delta L/2\gamma^2 c)$. Setting $Z_R = L$, we get

$$\eta = 8a_q(I/2\pi I_A \gamma G\Delta)^{1/2}, \tag{25}$$

where $I_A = ec/r_e \simeq 17{,}000A$ is the Alfven current. Note that this result is independent of L. This means that the short-pulse regime should be particularly attractive for small-scale FEL's. Of course, L must be sufficiently large to give enough small-signal gain to initiate lasing. Equation (25) must break down for large values of $\eta(N_s < 1)$, and is invalid when $N_s > N$. Equation (25) scales as $\gamma^{-1/2}$ or $\omega_s^{-1/4}$, which seems favorable for short-wavelength operation. However, low small-signal gain, large losses, and large dispersion are serious problems at short wavelengths.

Equation (25) is too crude to provide any information on the effects of chirping. However, it is easily shown that, aside from small differences in the diffractive factor $1 + i(z - z_0)/Z_R$, the FEL dynamical Eqs. (6)-(8) for $\alpha > 0$ are mathematically nearly equivalent to the equations for $\alpha = 0$. This equivalence is easily seen when Eqs. (6)-(8) are written in terms of the variables ψ, ϕ, ϕ_0, and $\tilde{E}_s$. The only difference is that the current $I(\phi_0)$ is replaced by $I(\phi_0)\exp(\alpha\phi_0/4\pi N)$. For $\alpha = 0.1$

the effective current increase is about 8%, which, according to Eq. (25), should increase η by a factor of 1.04. This is much less than the increase in η which is found in the computer simulations. Apparantly the explanation for the beneficial effects of chirping is not to be found solely by consideration of FEL dynamics within the wiggler.

The remaining effect of chirping is that cavity detuning tends to push the optical pulse below resonance as it is pushed forward. It is plausible that this would increase the efficiency, since electrons well above resonance have further to fall in the ponderomotive buckets. This suggests that efficiency enhancement might also be obtained with a uniform wiggler, unchirped electron micropulses, but a gradual increase in electron energy over the macropulse.

The wide spectral bandwidth of short optical pulses means that they can interact resonantly with a wide distribution of electron energies. Thus, the short-pulse regime of the FEL may be relatively insensitive to energy spread, at least in the saturated regime.

REFERENCES

1. G. T. Moore, Nucl. Instr. and Meth. **A272** (1988) 302.

2. G. T. Moore, Phys. Rev. Letters **60** (1988) 1825.

3. N. M. Kroll, P. L. Morton, and M. N. Rosenbluth, in *Free-Electron Generators of Coherent Radiation*, edited by S. F. Jacobs et al., Physics of Quantum Electronics, Vol. 7, (Addison-Wesley, Reading, MA, 1980), p. 89.

4. H. Al-Abawi, G. T. Moore, and M. O. Scully, Phys. Rev. A **24** (1981) 3143.

5. G. T. Moore and M. O. Scully, Phys. Rev. A **21** (1980) 2000.

6. H. Al-Abawi, F. A. Hopf, G. T. Moore, and M. O. Scully, Opt. Commun. **30** (1979) 235.

7. N. M. Kroll and M. N. Rosenbluth, in Ref. 3, p. 147.

8. J. C. Goldstein, B. E. Newnam, R. W. Warren, and R. L. Sheffield, Nucl. Instr. and Meth. **A250** (1986) 4.

Table 1. Synopsis of results of computer experiments with linear wavelength chirp and taper. Numbers in parentheses signify multiplication by powers of ten. Maximal gain is ill-defined for cases where the initial start-up is dominated by noise, since large fluctuations occur in the first few passes.

α_q	α_s	A_0	δ	$\ell(\mu m)$/ Pass Nos.	Maximal Gain (%)/ Pass No.	Gain (%) on Pass 40/80	Maximal Efficiency (%)/Pass No.
-0.02	0.02	1.	.001	10./1-80	94.1/5	13.2/3.3	1.74/38
"	"	"	"	2./41-80	"	13.2/5.1	2.13/80
"	"	"	"	0.5/41-120	"	13.2/5.6	3.53/119
-0.05	0.05	"	"	10./1-40	2.9/2	3.9(-5)	2.2(-7)/2
"	"	"	"	0.5/1-340	26.1/27	23.7/16.6	4.91/337
"	"	"	"	0/341-380	"	"	5.21/378
-0.1	0.1	"	"	0.5/1-40	4.4/30	4.4	2.2(-7)/40
-0.08	0.08	"	"	0.5/1-120	11.8/78	9.5/11.8	2.8(-5)/120
"	"	"	"	0.25/1-40	10.8/40	10.8	1.95(-7)/40
-0.06	0.1	"	"	0.5/1-40	9.8/40	9.8	1.5(-7)/40
-0.02	"	"	"	0.5/1-400	18.9/34	18.7/14.8	4.13/395
"	0.14	"	"	0.5/1-40	10.3/40	10.3	1.8(-7)/40
0	0	"	"	0.5/1-160	144/2	21.1/7.8	4.14/159
"	"	"	"	0/161-200	"	"	5.02/199
-0.05	0.05	"	"	5./1-240	29.8/44	29.6/26.4	1.53/112
"	"	"	"	10./1-200	29.0/58	22.8/28.9	1.18/121
-0.02	0.02	"	"	10./1-120	210/14	9.5/7.9	2.29/100
"	"	"	"	40./1-40	42.5/32	11.7	4.6(-6)/40
"	"	"	"	30./1-40	69.9/12	6.8	3.2(-5)/27
0	0	"	"	"	274/7	6.6	0.57/40
0	0.05	"	"	0.5/1-280	75.6/6	23.9/10.2	6.40/269
"	"	"	"	0/241/280	"	"	6.82/278
"	0.1	"	"	0.5/1-200	26.9/22	22.6/15.3	1.68/200
0.05	0.05	"	"	0.5/1-240	145/2	21.7/8.4	6.99/235
"	"	"	"	0/201-320	"	"	7.82/315
0.1	0.1	"	"	0.5/1-200	145/2	21.5/8.9	7.03/200
"	"	"	"	0/201-240	"	"	7.85/240
"	"	"	"	0.05/241-320	"	"	8.13/279
"	"	"	"	0.5/201-240	"	"	7.66/239
"	"	"	"	0/241-320	"	"	7.93/268
"	"	"	0.	0.05/1-40	144/2	20.1	6.6(-2)/40
"	"	"	"	0.5/1-40	145/2	21.5	0.105/40
"	"	1.(-6)	.001	0.5/1-600	—	24.8/17.3	5.85/561
"	"	"	0.	0.5/1-40	143/2	22.8	1.15(-13)/40
"	"	10.	.001	0.5/1-200	145/2	12.2/6.5	7.48/189
"	"	"	"	0/121-160	"	"	7.10/160
0.2	0.2	1.	"	0.5/1-200	142/2	19.7/9.9	4.23/192
0.1	0.1	"	"	1.0/1-160	146/2	22.0/9.1	6.99/158
"	"	"	"	0.25/1-160	144/2	20.8/8.7	3.84/160
0.05	0.05	1.(-6)	.01	0.5/1-120	—	26.1/17.1	0.73/120
0.1	0.1	"	"	0.5/1-480	—	25.8/17.3	6.56/329
0	0	1.	.001	10./1-40	146/2	6.9	1.47/32
"	"	"	"	0.5/41-80	"	6.9/5.6	2.32/77

FIGURE CAPTIONS

Fig. 1. Single-pass small-signal gain for long electron pulse with error-function chirp and uniform wiggler ($\epsilon_s = 2$, $\alpha_s = 0.25$, $\tau_c = 19.0$ psec, $\tau_s = 19.7$ psec, $T_e = T_s = 6.171$ psec).

Fig. 2. Efficiency growth for a short pulse with an error-function chirp and an untapered wiggler.

Fig. 3. Pulse characteristics on pass 280 for the example of Fig. 2. Upper left: electron energy (solid line) and current (dashed line, peak = 100 A). Lower left: Efficiency/bin is the fractional part of the electron energy extracted, and does not weight the electron current. Lower right: Resonant wave number ω_s/c (solid line) and time derivative of the total optical phase divided by c (dashed line).

Fig. 4. Efficiency growth for several examples combining linear wavelength chirp and taper for the short electron pulse. The cavity length detuning is $\ell = 0.5\mu m$ (solid lines) or $\ell = 0$ (dashed lines), except where otherwise indicated.

Fig. 5. Pulse evolution for $\alpha_s = \alpha_q = 0.1$, the "best case" of Fig. 4. $\mathcal{E}_e$ denotes the incident electron pulse kinetic energy. $\mathcal{E}_s$ denotes the optical pulse energy (upper left, incident energy at $z = 0$; elsewhere, energy at $z = L$). η denotes the efficiency. Curves have the same meaning as in Fig. 3.

Fig. 6. Continued evolution of the optical power for the case shown in Fig. 5.

Fig. 7. Further evolution of the optical and electron pulses for the case shown in Figs. 5 and 6.

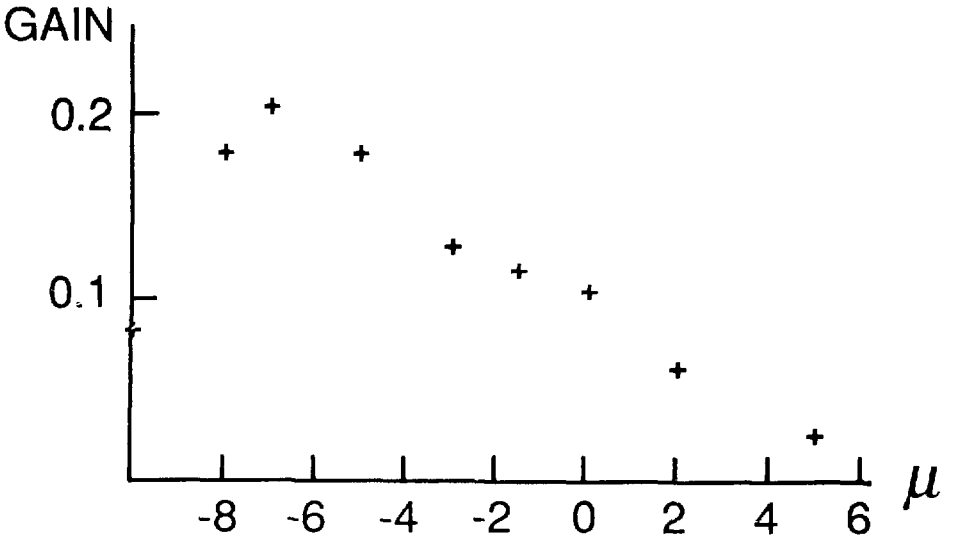
GAIN
0.2
0.1
-8
-6
-4
-2
0
2
4
6
μ

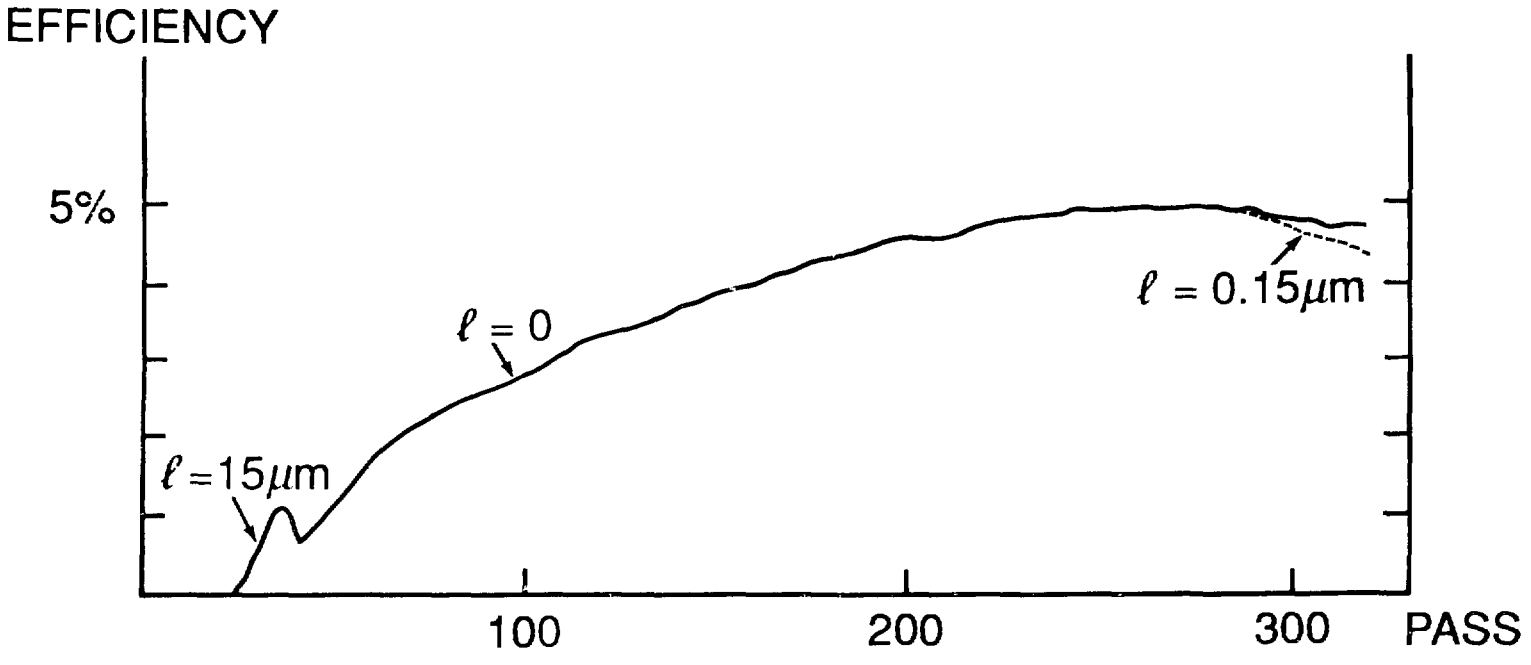
EFFICIENCY
5%
ℓ = 0
ℓ = 0.15μm
ℓ = 15μm
100
200
300
PASS

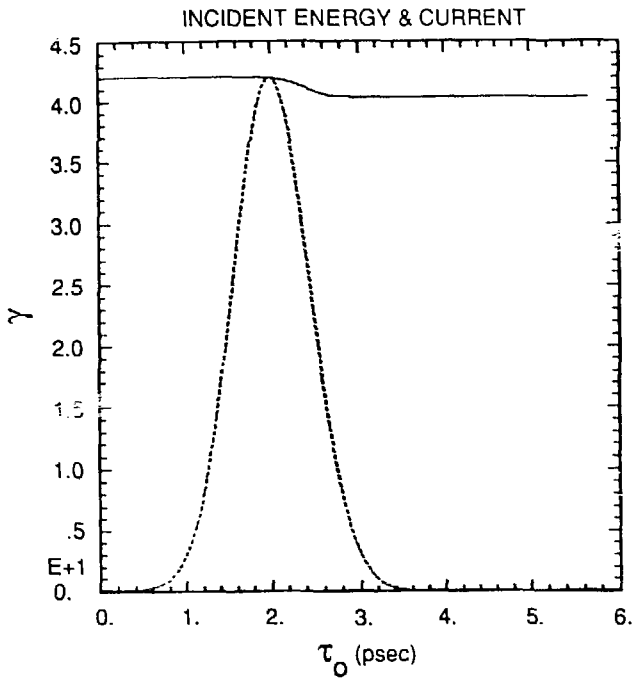
INCIDENT ENERGY & CURRENT
γ
4.5
4.0
3.5
3.0
2.5
2.0
1.5
1.0
.5
E+1
0.
0.
1.
2.
3.
4.
5.
6.
τo (psec)

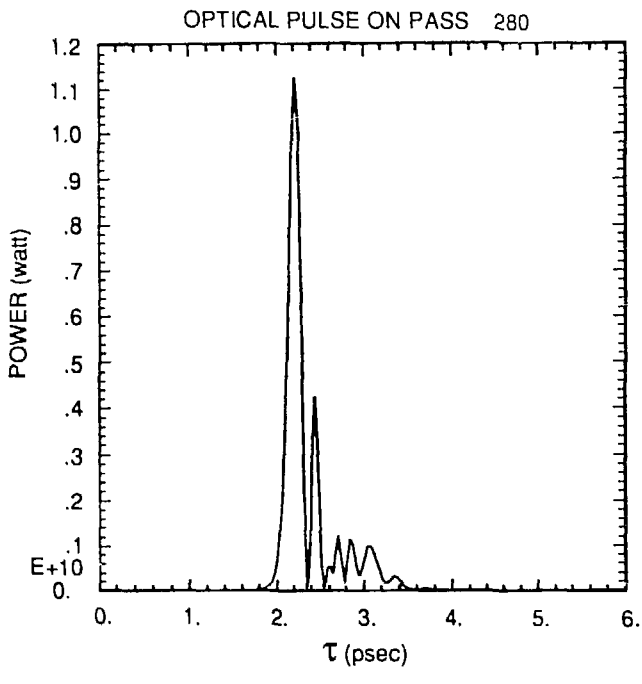
OPTICAL PULSE ON PASS 280
POWER (watt)
1.2
1.1
1.0
.9
.8
.7
.6
.5
.4
.3
.2
.1
E+10
0.
0.
1.
2.
3.
4.
5.
6.
τ (psec)

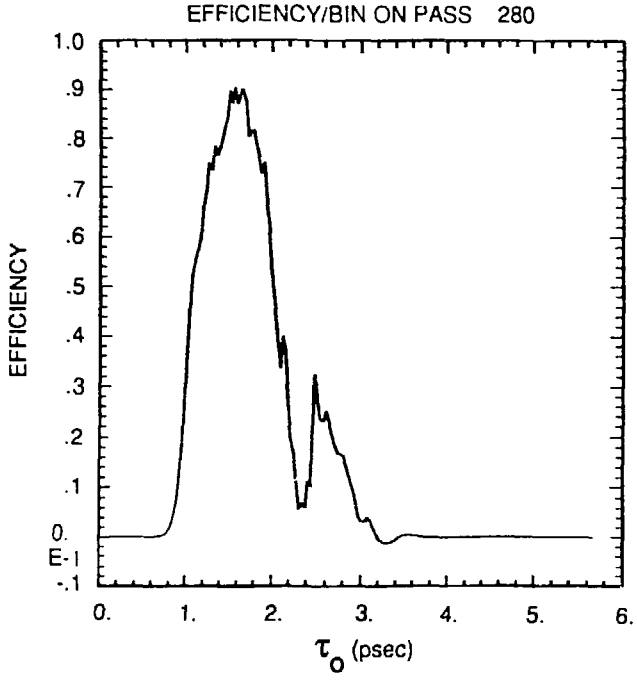
EFFICIENCY/BIN ON PASS 280
EFFICIENCY
1.0
.9
.8
.7
.6
.5
.4
.3
.2
.1
0.
E-1
-.1
0.
1.
2.
3.
4.
5.
6.
τo (psec)

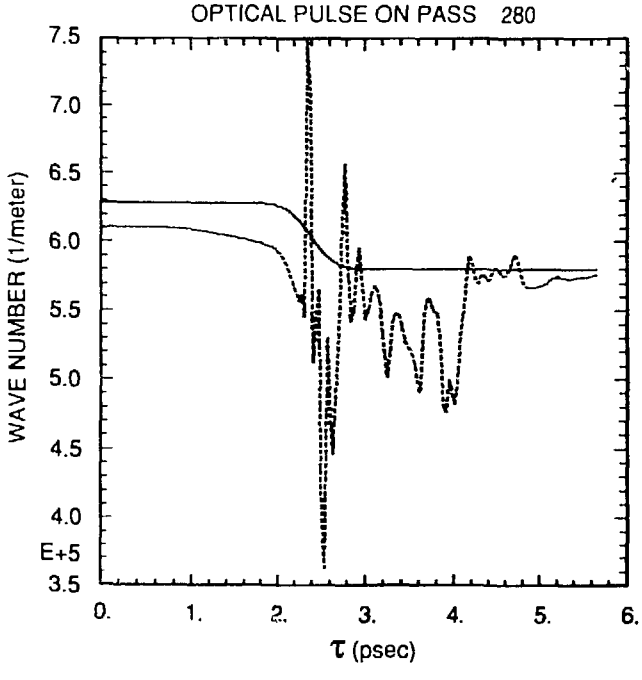
OPTICAL PULSE ON PASS 280
WAVE NUMBER (1/meter)
7.5
7.0
6.5
6.0
5.5
5.0
4.5
4.0
E+5
3.5
0.
1.
2.
3.
4.
5.
6.
τ (psec)

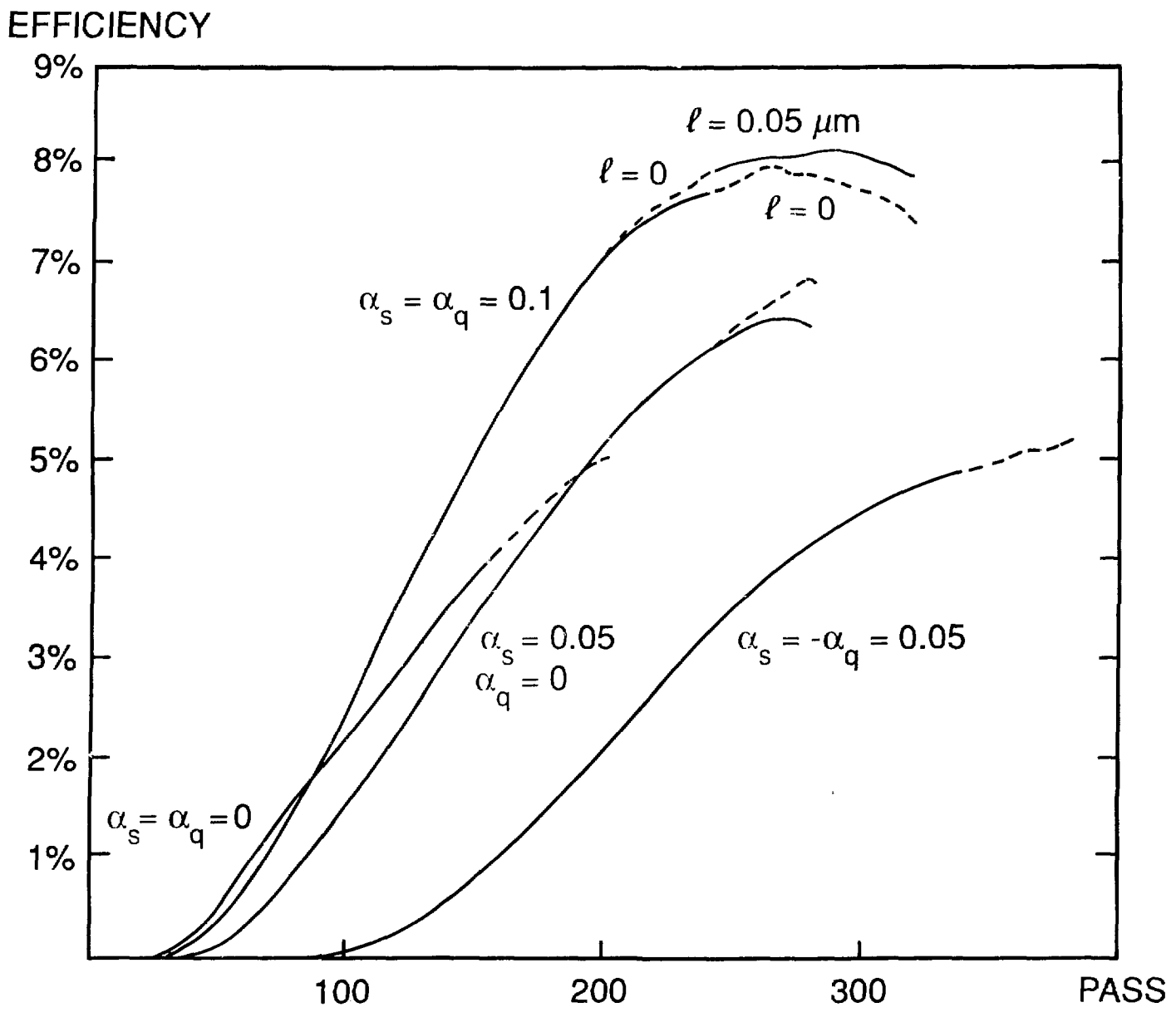
EFFICIENCY
9%
8%
7%
6%
5%
4%
3%
2%
1%
ℓ = 0.05 μm
ℓ = 0
ℓ = 0
$\alpha_s = \alpha_q = 0.1$
$\alpha_s = 0.05$
$\alpha_q = 0$
$\alpha_s = -\alpha_q = 0.05$
$\alpha_s = \alpha_q = 0$
100
200
300
PASS

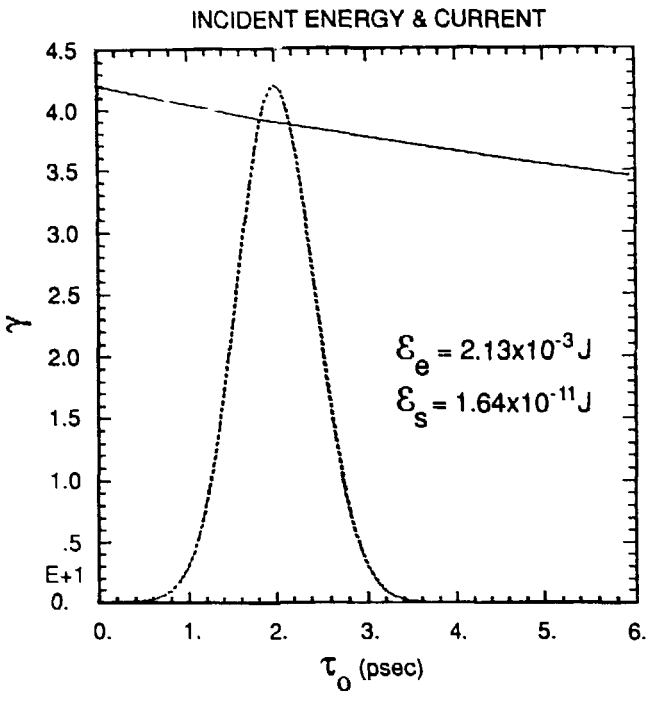
INCIDENT ENERGY & CURRENT
γ
4.5
4.0
3.5
3.0
2.5
2.0
1.5
1.0
.5
E+1
0.
0.
1.
2.
3.
4.
5.
6.
τ_o (psec)
$\mathcal{E}_e = 2.13 \times 10^{-3}$ J
$\mathcal{E}_s = 1.64 \times 10^{-11}$ J

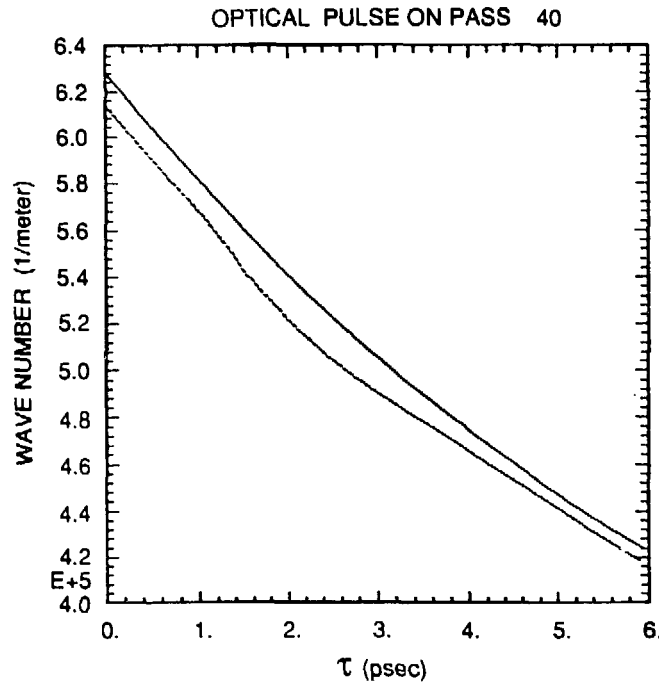
OPTICAL PULSE ON PASS 40
WAVE NUMBER (1/meter)
6.4
6.2
6.0
5.8
5.6
5.4
5.2
5.0
4.8
4.6
4.4
4.2
E+5
4.0
0.
1.
2.
3.
4.
5.
6.
τ (psec)

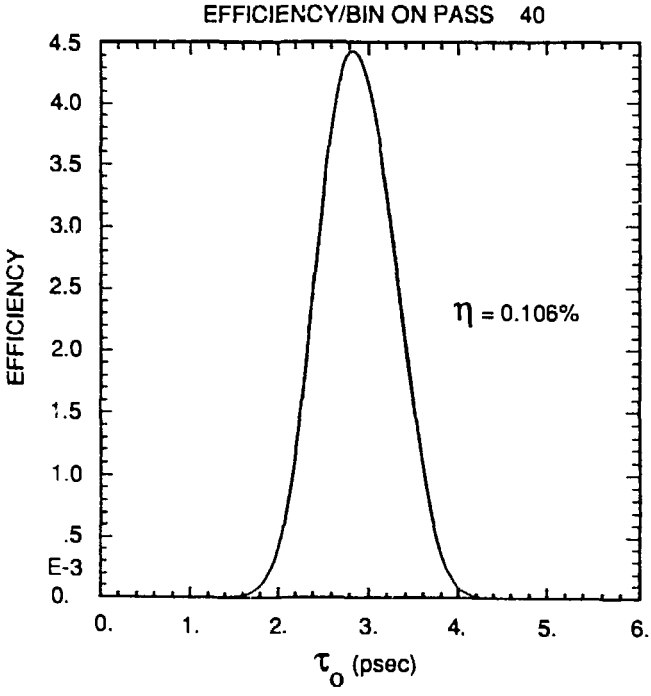
EFFICIENCY/BIN ON PASS 40
EFFICIENCY
4.5
4.0
3.5
3.0
2.5
2.0
1.5
1.0
.5
E-3
0.
0.
1.
2.
3.
4.
5.
6.
τ_o (psec)
$\eta = 0.106\%$

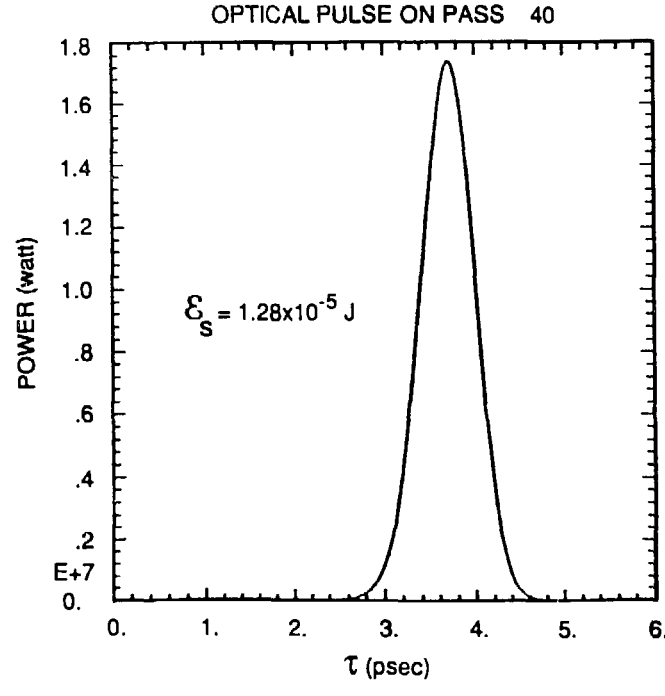
OPTICAL PULSE ON PASS 40
POWER (watt)
1.8
1.6
1.4
1.2
1.0
.8
.6
.4
.2
E+7
0.
0.
1.
2.
3.
4.
5.
6.
τ (psec)
$\mathcal{E}_s = 1.28 \times 10^{-5}$ J

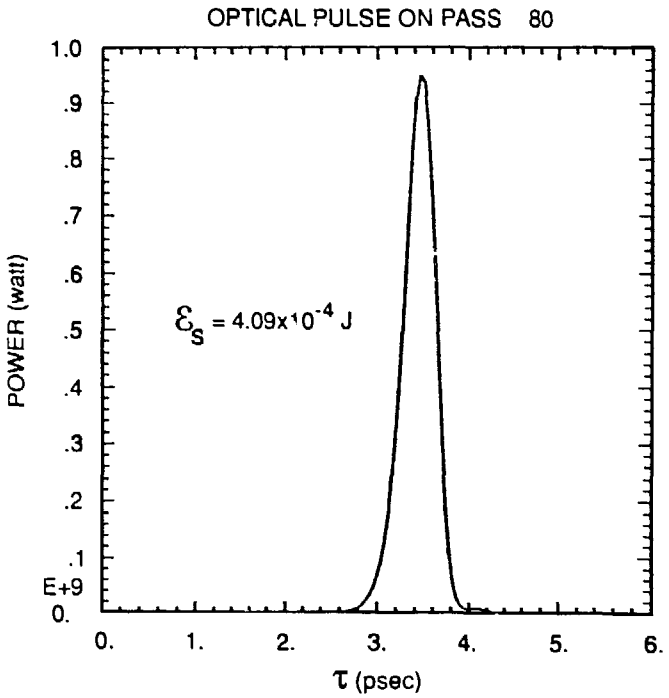
OPTICAL PULSE ON PASS 80
POWER (watt)
1.0
.9
.8
.7
.6
.5
.4
.3
.2
.1
E+9
0.
$\mathcal{E}_s = 4.09 \times 10^{-4}$ J
0. 1. 2. 3. 4. 5. 6.
τ (psec)

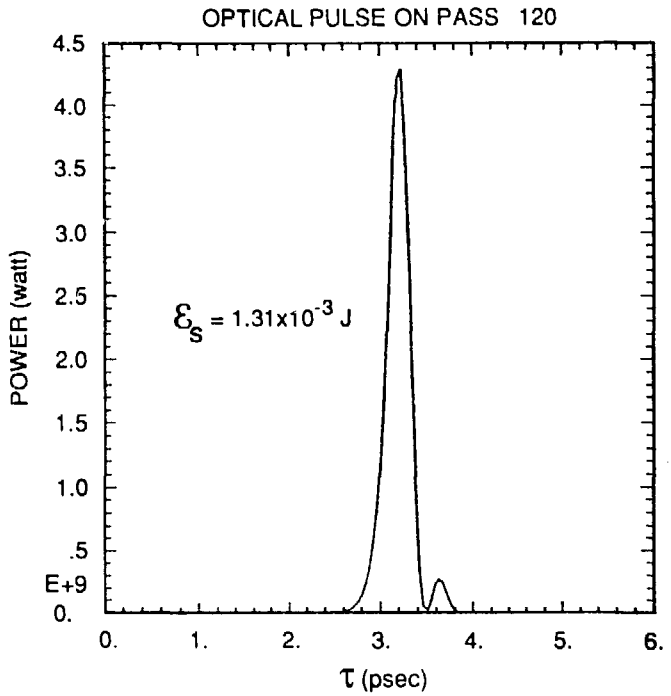
OPTICAL PULSE ON PASS 120
POWER (watt)
4.5
4.0
3.5
3.0
2.5
2.0
1.5
1.0
.5
E+9
0.
$\mathcal{E}_s = 1.31 \times 10^{-3}$ J
0. 1. 2. 3. 4. 5. 6.
τ (psec)

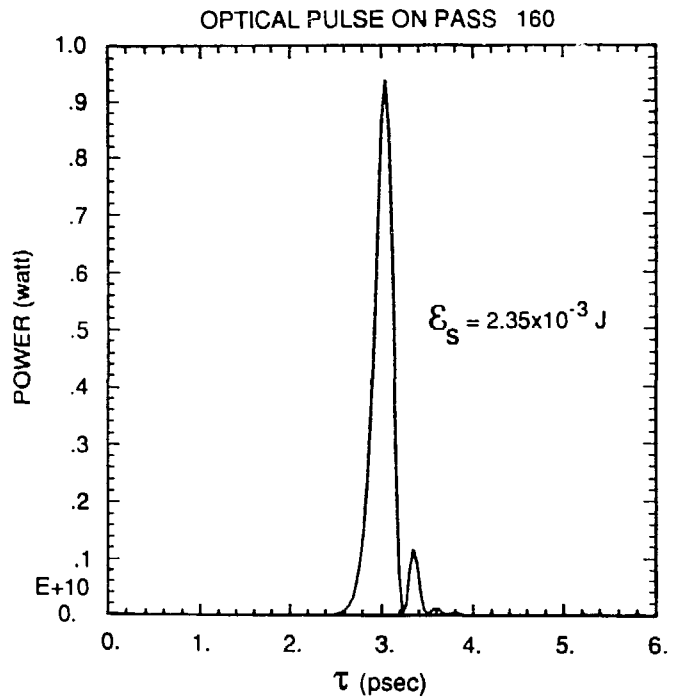
OPTICAL PULSE ON PASS 160
POWER (watt)
1.0
.9
.8
.7
.6
.5
.4
.3
.2
.1
E+10
0.
$\mathcal{E}_s = 2.35 \times 10^{-3}$ J
0. 1. 2. 3. 4. 5. 6.
τ (psec)

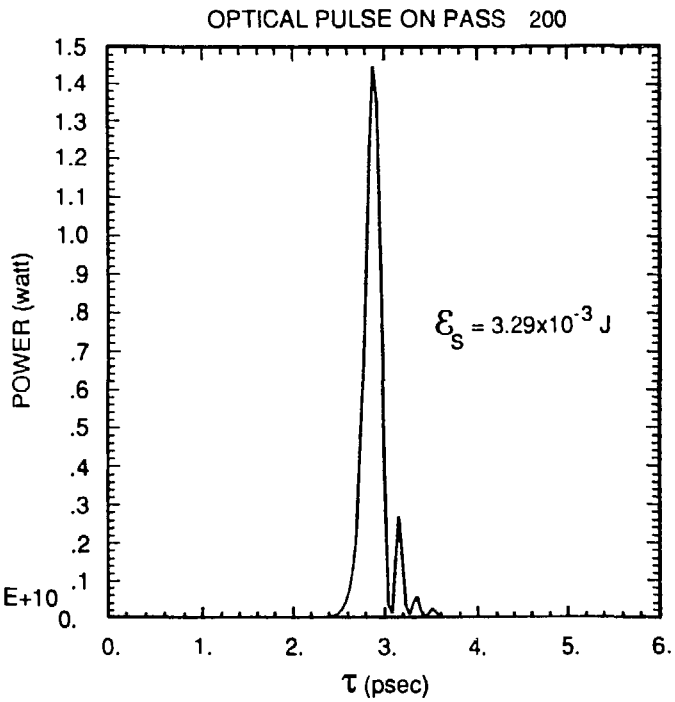
OPTICAL PULSE ON PASS 200
POWER (watt)
1.5
1.4
1.3
1.2
1.1
1.0
.9
.8
.7
.6
.5
.4
.3
.2
.1
E+10
0.
$\mathcal{E}_s = 3.29 \times 10^{-3}$ J
0. 1. 2. 3. 4. 5. 6.
τ (psec)

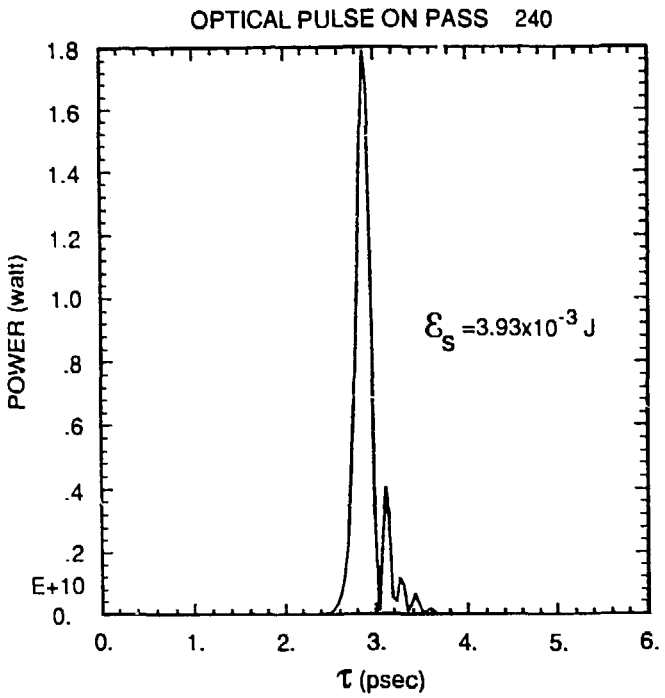
OPTICAL PULSE ON PASS 240
POWER (watt)
1.8
1.6
1.4
1.2
1.0
.8
.6
.4
.2
E+10
0.
$\mathcal{E}_s$ =3.93x10^{-3} J
0. 1. 2. 3. 4. 5. 6.
τ (psec)

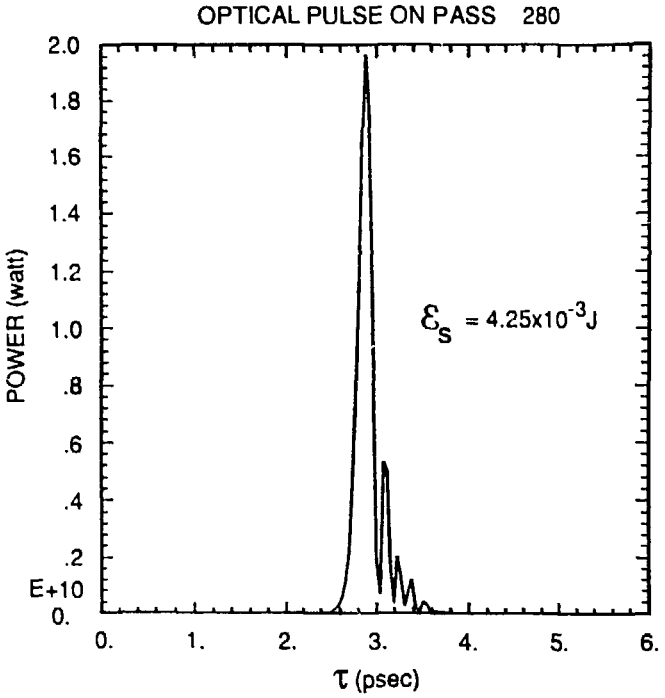
OPTICAL PULSE ON PASS 280
POWER (watt)
2.0
1.8
1.6
1.4
1.2
1.0
.8
.6
.4
.2
E+10
0.
$\mathcal{E}_s$ = 4.25x10^{-3}J
0. 1. 2. 3. 4. 5. 6.
τ (psec)

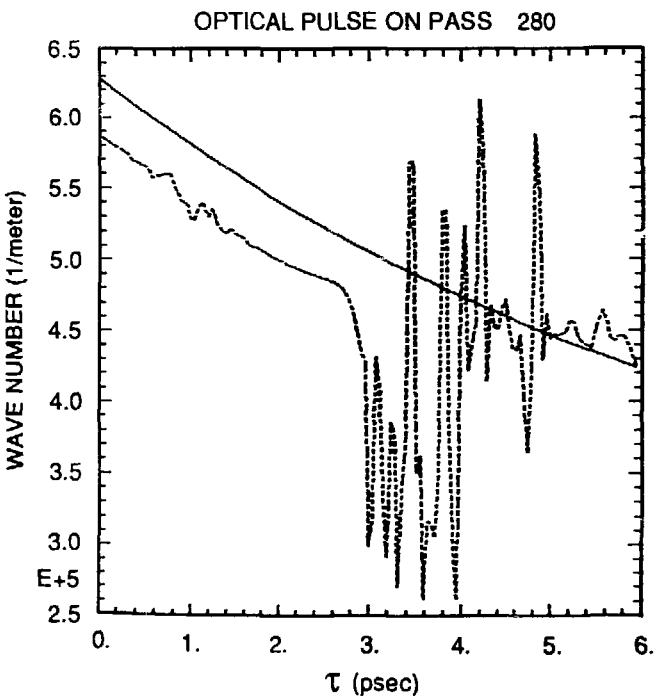
OPTICAL PULSE ON PASS 280
WAVE NUMBER (1/meter)
6.5
6.0
5.5
5.0
4.5
4.0
3.5
3.0
E+5
2.5
0. 1. 2. 3. 4. 5. 6.
τ (psec)

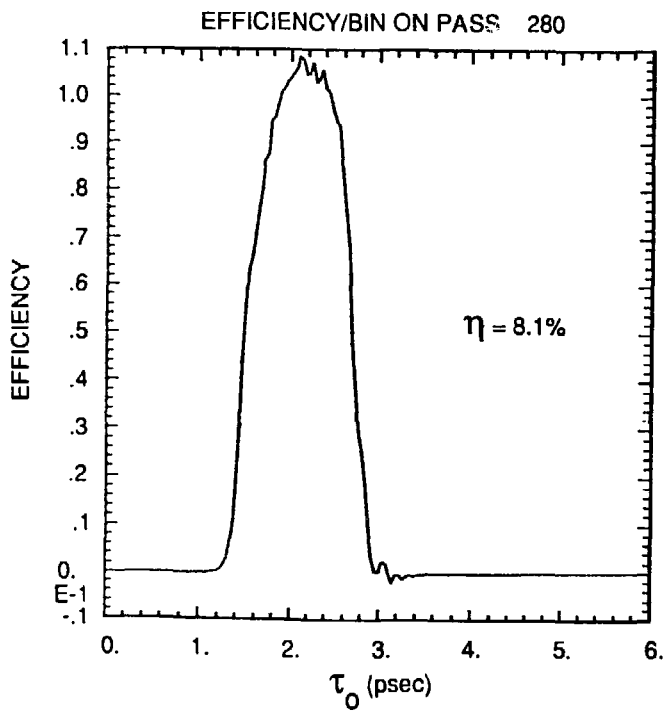
EFFICIENCY/BIN ON PASS 280
EFFICIENCY
1.1
1.0
.9
.8
.7
.6
.5
.4
.3
.2
.1
0.
E-1
-.1
η = 8.1%
0. 1. 2. 3. 4. 5. 6.
τ$_0$ (psec)